Lattice dynamics and phonon line shapes in ^{36}Ar at high temperatures

J. Eckert
Physics Division, Los Alamos National Laboratory, University of California, Los Alamos, New Mexico 87545

R. W. Youngblood
Nuclear Energy Department, Brookhaven National Laboratory, Upton, New York 11973-5000
(Received 15 November 1985)

The inelastic neutron scattering technique has been used to measure phonon frequencies and phonon line shapes in ^{36}Ar at temperatures of 81 K [lattice constant $a=5.465(2)$ Å] and 55 K [$a=5.440(2)$ Å] primarily along the [100] and [110] directions. The 81-K data combined with earlier results for small wave vector by Fujii *et al.* were fitted to a force-constant model. Detailed comparisons are made of the observed phonon line shapes with those computed from the self-consistent harmonic approximation with added cubic anharmonicity (Glyde and co-workers) and molecular-dynamics simulations (Hansen and Klein). The agreement at high temperatures though still quite satisfactory, was found to be not as good as at low temperatures.

I. INTRODUCTION

The lattice dynamics of rare-gas solids have been the subject of extensive studies[1] since they represent ideal systems for testing advanced theories of lattice dynamics as well as fine details of the interatomic potential of van der Waals atoms. At low temperatures it is therefore possible to predict the phonon dispersion curves of rare-gas solids extremely accurately.[2,3] At high temperatures, however, the situation is considerably less satisfactory. Typically the neutron scattering experiments performed at temperatures near the melting point report only the small q portions of the phonon dispersion relations, i.e., the elastic constants.[4,5] One reason for this is that even for the heaviest rare-gas solids anharmonicity becomes significant at high temperatures, and as a result, phonon line shapes at large values of Q are asymmetrically broadened by multiphonon processes. It can then be difficult to discern the "true" one-phonon frequency from the observed spectrum. Furthermore, in extreme cases, i.e., for very large anharmonicity, multiphonon processes may become dominant and a one-phonon frequency can no longer be defined.

The earliest detailed calculations of phonons in solid argon over a wide range of temperatures, that included lifetimes as well as frequencies, were carried out by Bohlin and Hogberg[6] using a quasiharmonic perturbation theory. More recently, however, significant progress has been made in calculating theoretical phonon line shapes for highly anharmonic systems using self-consistent phonon theories[7-10] and molecular-dynamics simulations.[11] This effort was necessitated by the experimental work on solid helium[3,12] which is highly anharmonic under all conditions short of very high densities. Thus, for example, the self-consistent harmonic approximation with added cubic terms (referred to as SCH + C by Glyde and co-workers[7]) has been used to compute phonon line shapes to compare with neutron scattering experiments. This calculation includes contributions from two-phonon processes and interference terms between one- and two-phonon scattering. The latter are responsible for the apparent oscillations of the phonon intensities about the harmonic value that are observed[13] as a function of momentum transfer Q, while both terms can provide asymmetry in the phonon line shapes. This theory has been applied to solid helium at normal[3,7] and high densities,[9] to solid neon[8] at low temperatures, and more recently to argon by Glyde and Smoes[10] (referred to as GS subsequently) at various temperatures. In general the SCH + C approximation gives very good agreement for the one-phonon frequencies including their temperature dependence and qualitatively reproduces the broad shoulders observed in the line shapes of high-energy longitudinal phonons.

For higher temperatures, however, the effectiveness of either the self-consistent phonon theories or the molecular-dynamics (MD) simulations in accounting for experimentally observed phonon line shapes is much more difficult to assess because of the lack of experimental data. In particular, the neutron scattering work of Fujii *et al.*[14] contains line-shape data for only one phonon, a longitudinal mode at $Q=(2.5,0,0)$, as a function of temperature. It shows a dramatic broadening as the temperature is increased from 55 to 75 K (Fig. 7 in Ref. 14) which has not been reproduced in either the SCH + C calculation[10] or the MD simulation.[11] For phonons with frequencies greater than approximately twice that of the first maximum in the density of states (viz., when two-phonon processes become important) both types of calculations do give line shapes which broaden strongly with temperature.

Further progress in applying either self-consistent phonon or MD calculations to the lattice dynamics of simple solids up to temperatures near the melting point is, of course, critically dependent on rectifying the lack of appropriate phonon dispersion and line-shape data mentioned above. We have therefore undertaken to complete the measurement of phonon dispersion relations in ^{36}Ar close to the melting point ($T_m=83.7$ K), for which the small wave-vector portion is already contained in the work of Fujii and co-workers.[14] Following a brief discussion of the experimental details, we will present phonon

dispersion relations measured at 81 K as well as some phonon frequencies at 55 K and Born—von Kármán force constant fits to the data. In this and the final section on phonon line shapes, this new data will, to the extent possible, be compared with the two types of theoretical efforts referred to above.

II. EXPERIMENTAL DETAILS

The growth of single crystals of rare-gas solids for neutron scattering experiments has been described at some length in previous papers[15] on this subject and will therefore not be repeated here. We utilized these techniques to grow from the melt a single crystal of ^{36}Ar in a Kapton (polypyromelitinide) cell of 6 mm diam and 25 mm height. After completion of the growth the sample was held at 8 K and a single crystal of approximately $\frac{1}{4}$ the size of the sample cell was found with a $[11\bar{2}]$ axis perpendicular to the scattering plane. It was utilized for measurements of some L[111] and T[111] phonons. During these measurements (i.e., within the first 24 h after completion of the crystal growth) this grain apparently annealed into another one with the result that now a single crystal with a [001] axis vertical almost completely filled the sample cell. The rest of the experiment was therefore limited to measuring phonons along [100] and [110] directions, and only some of the data taken in the [111] direction was useful. Several of the phonons used as examples by GS could therefore not be measured for comparison with theory. The crystal mosaic at 81 K was approximately 20 min full width at half maximum (FWHM). The quality of the crystal was checked routinely every few hours by scanning Bragg peaks as well as selected "standard" phonons to ensure that the observed phonon line shapes were not affected by a possible deterioration of the crystal. However, the crystal retained its mosaic at a given temperature. After completion of data collection at 81 K the crystal was cooled at the rate of about 1.5 K/h to 55 K in an attempt to observe lineshape changes of several phonons as a function of temperature.

Measurements of the phonon groups were performed on a triple-axis spectrometer at the Brookhaven National Laboratory High-Flux Beam Reactor in the constant-Q mode of operation. Monochromator and analyzer were pyrolytic graphite and higher-order contamination was removed by a graphite filter after the sample. All scans were made by holding the final neutron energy fixed at 13.7 meV. Horizontal collimations were 20′-20′-40′-40′ (FWHM) for in-pile, monochromator sample, sample analyzer, and analyzer detector, respectively. The energy resolution at zero energy transfer for this configuration is 0.57 meV (FWHM).

Since the work of Fujii *et al.*[14] includes phonons for all branches at 82 K up to reduced wave vectors of 0.2, we did not repeat their measurements except for control purposes. Their data were also included in the force-constant fits to be discussed below. Instead the emphasis of this work was to observe the line shapes of some of the broad, high-energy phonons.

In order to determine values for the phonon energies one or more Gaussians were fitted to the observed profiles, which were sometimes complicated either by the multiphonon effects mentioned above or by picking up contributions from out-of-plane phonons because of the rather coarse vertical collimation used. In the former case the fitting procedure was guided by the theoretical results (e.g., Figs. 10 and 11 of GS) which explicitly show the two-phonon contribution at high energies.

III. RESULTS AND DISCUSSION

A. Phonon dispersion relation at 81 K

The experimental phonon frequencies in ^{36}Ar at both 81 and 55 K are given in Table I along with their fitting errors. Phonon energies for $\zeta = q(a/2\pi) < 0.2$ are listed in Table I of the work of Fujii *et al.* The measured lattice constant a was 5.465(2) Å at 81 K and 5.440(2) Å at 55 K. Both the present data at 81 K (solid circles) and some of the data from Fujii *et al.* (solid squares) are displayed in Fig. 1 giving the dispersion curves of ^{36}Ar near the melting point. The T_2[110] branch has a polarization vector perpendicular to the scattering plane of the present experiment and could therefore not be directly observed. In two longitudinal scans, however, a contribution from this branch was present on account of the relaxed vertical collimation used. This hypothesis was checked with a computer program[16] which uses force constants to calculate full dispersion surfaces and then generates a resolution-broadened line shape for a desired constant-Q scan. These two points on the T_2[110] branch are thus shown as open circles in Fig. 1 and their position is to be regarded as somewhat less certain. For all the other data the uncertainties are no greater than the size of the points shown.

A Born—von Kármán force-constant model was fit to the combined high-temperature data and the resulting parametrization is shown as a dashed line in Fig. 1. For the [100] direction our data are compared with the results of the SCH + C calculation for $T = 75$ K by GS (solid line in Fig. 1 and in Fig. 4 of GS). While the agreement in this case is still satisfactory, it is not nearly as good as at 10 K (Fig. 2 of Ref. 14). The relative disagreement shown for the L[100] branch is most likely the result of the increased importance of anharmonicity at the higher temperatures.

The results of the force-constant fit are given in Table II and again compared with that at 10 K. The "best" model for the combined high-temperature data was for axially symmetric forces to third neighbors. General force models were not determined well enough because of the lack of data along some branches and the fact that the L-point phonons could not be measured as discussed above. Inclusion of further neighbors resulted in only marginally better fits and was therefore not considered significant. It is apparent from the force-constant values presented in Table II that the nature of the interatomic forces has not changed markedly with temperature, except perhaps for a slight increase in noncentral character as evidence by a larger nonzero value of k_{1ZZ}. In fact, when the axially symmetric constraints are removed in fitting the high-temperature data, k_{1ZZ} becomes very large though poorly determined. The force constants from

TABLE I. Experimental phonon frequencies in solid ^{36}Ar at 81 and 55 K (in meV). Errors given are statistical only.

ζ	81 K	55 K		81 K	55 K
	T		[ζ00]	L	
0.2				2.18(5)	
0.3	2.13(2)	2.41(1)		2.96(3)	
0.4				4.01(7)	4.49(6)
0.5	3.13(3)	3.84(2)			
0.6				5.66(8)	6.04(3)
0.75	4.52(2)	5.04(2)			
0.8				6.96(7)	7.21(5)
1.0	4.89(5)	5.39(3)		7.46(23)	
	T_1		[$\zeta\zeta$0]	L	
0.15				2.40(1)	
0.2	1.276(7)			3.14(2)	3.54(4)
0.3				4.58(3)	5.04(3)
0.4	2.55(2)				
0.5				6.37(7)	6.96(3)
0.6	3.78(2)	4.19(2)			
0.7				6.03(7)	6.55(2)
0.8	4.67(3)	5.08(3)			
	T		[$\zeta\zeta\zeta$]	L	
0.1				2.14(5)	
0.2	1.79(3)			4.20(5)	
0.25				4.84(5)	
0.4				6.61(27)	
0.5				7.09(13)	

Table II were used to compute[17] the phonon density of states shown in Fig. 2, where the curve for 10 K is simply a reconstruction of Fig. 3 in the work of Fujii *et al.*

B. Phonon line shapes

Since most of the recent theoretical efforts on the lattice dynamics of rare-gas crystals have been concerned with the detailed form of the dynamic structure factor, we will present in this section a number of relevant experimental phonon line-shape measurements for qualitative comparison with the work of Glyde and Smoes.[10] Where possible we will also make reference to the MD simulations of Hansen and Klein.[11] The latter results, however, typically show much secondary structure (presumably because of statistical fluctuations) so that line-shape comparisons are somewhat more difficult. Most of our data were taken to bear on the question of the temperature dependence of the phonon line shapes with less emphasis on their Q dependence. The latter has already been addressed at length in previous work on other rare-gas solids.[12] For longitudinal phonons propagating in the [111] direction in fcc He, for example, the SCH + C approximation was used to demonstrate, at least qualitatively, that it is difficult to extract precise one-phonon energies from the observed scattering at large enough momentum and energy transfers because of a substantial amount of two-phonon scattering (Fig. 3 in Ref. 12). In addition to the Q dependence of the phonon line shapes, Collins and Glyde also addressed the isochoric temperature shift of the phonon frequencies in fcc He. The latter was a unique aspect of the high-pressure neutron scattering work since the crystal could be held at constant volume. For this strictly anharmonic effect the SCH + C theory gave good agreement (viz., within a factor of 2) with the

TABLE II. Interatomic force constants (in dyn cm^{-1}) of solid ^{36}Ar at 10 K (Ref. 14) and at 51 K. The values at 10 K are for a three-neighbor, general force model (model 2 in Table II of Ref. 14), while the data at 81 K were fitted with a three-neighbor axially symmetric model. In the latter case one has the constraints $k_{1XX}-k_{1ZZ}=k_{1XY}, k_{3XX}-k_{3YY}=3k_{3YZ}$ and $2k_{3XX}-2k_{3YY}=3k_{3XZ}$.

Force constant	10 K	81 K
k_{1XX}	605(10)	503(33)
k_{1ZZ}	5(14)	−16(16)
k_{1XY}	633(18)	520(44)
k_{2XX}	−24(22)	−14(21)
k_{2YY}	−3(8)	−6(22)
k_{3XX}	−5(8)	−31(11)
k_{3YY}	0(2)	−9(4)
k_{3XZ}	−2(4)	−7(3)
k_{3YZ}	0(4)	−15(6)

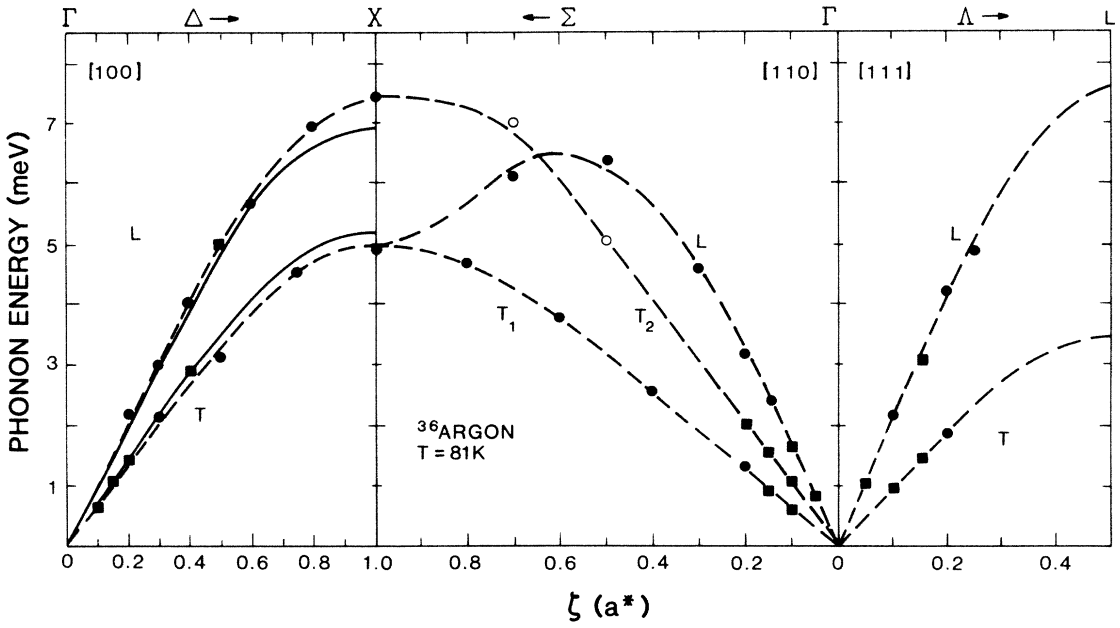

FIG. 1. Phonon dispersion relations for solid ^{36}Ar at 81 K. Phonons observed in this work are shown as circles, while data from Fujii *et al.* (Ref. 14) are indicated as squares. The dashed lines are force-constant fits to the data (see the text), and the solid line in the [100] direction are the results of the SCH + C calculation by Glyde and Smoes (Ref. 10).

experiment as well. The range of temperatures over which the fcc phase of He is stable is, however, rather narrow and detailed studies of the temperature dependence of the phonon line shapes were therefore not possible in that case.

In the work on ^{36}Ar, however, the discussion of the temperature dependence did include data (Fig. 13 in GS) of a longitudinal-acoustic (LA) phonon with $\mathbf{Q}/a^* = (2.5,0,0)$ for temperatures between 10 and 75 K. This phonon had a simple Gaussian line shape at low temperatures and showed a dramatic broadening in going from 55 to 75 K, which the subsequent SCH + C calculation could not produce satisfactorily. GS generally found the broadening of the phonon line shapes with temperature to be gradual with no abrupt changes in width. Only phonons with energies greater than about 6 meV showed complex line shapes at high temperatures because of a marked increase in the computed one-phonon width near that energy and the increased importance of two-phonon processes with temperature.

We would, therefore, like to present several sets of phonon groups measured at 55 and at 81 K for more complete comparisons with the calculations. Shown in Fig. 3 are two T[100] phonons with $q=0.75$ and at the zone boundary (X point) along with similar phonons computed from the SCH + C theory. The solid lines shown for the experimental data in Figs. 3–5 are the results of the fitting procedure described in Sec. II. The agreement appears to be very good, particularly if one considers that the calculations were performed at larger values of Q, i.e., near (0,2,2), whereas the measurements had to be done near (2,0,0). This may well explain the apparently greater widths obtained by GS.

The phonon group at the X point should also be compared with Fig. 16 of GS, which presents a comparison of the MD simulation of Hansen and Klein with the SCH + C theory. Again, it should be noted that the zone boundary point in this figure is at large Q, i.e., (2,1,1) versus (2,1,0) in our experiment. Nevertheless, it is apparent that both the line shape and the peak position given by the SCH + C calculation agrees better with experiment than does the MD simulation. The experimental frequency of 4.89 meV falls slightly below the SCH + C value (see Fig. 1) but well above the MD result (approximately 4.5 meV).

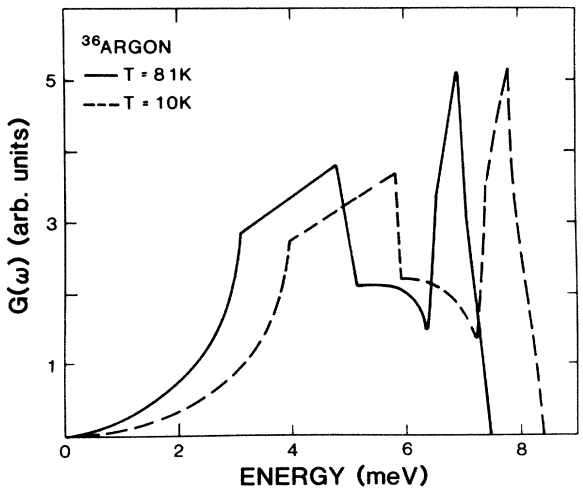

FIG. 2. Phonon density of states computed from force constants for ^{36}Ar at 10 K (Ref. 14) and 81 K (present work).

The broadening observed for some $L[100]$ phonons at high temperatures is shown in Fig. 4. These groups, with energies at or above 6 meV, appear to reflect the additional width from the increase in $\Gamma(\omega)$ in this energy range which the SCH + C theory predicts, when compared with the T[100] phonons at low energies. However, the change in width in going from 55 K to temperatures near the melting point is not nearly as large in our measurement as that observed for L(2.5,0,0) by Fujii *et al.*[14] The reason for this is not clear, but it could be related to crystal mosaic or different experimental conditions used, i.e., operation with E_i fixed as opposed to E_f fixed in this measurement. Again, the agreement with the SHC + C line shapes is qualitatively very good.

While the L[100] phonon with wave vector (2.8,0,0) (Fig. 4) does not show a significant asymmetry in the line shape resulting from multiphonon processes, the zone boundary mode L(3,0,0) has a pronounced shoulder on the high-energy side (Fig. 5). In order to display the experimental line shape for the phonon clearly a small peak on the low-energy side was fitted along with the rest of the phonon group and subsequently subtracted out. This peak has its origin in the relaxed vertical beam collimation used in the spectrometer, so that a portion of the T[100] mode at this zone boundary point can be detected. This subtraction should not have any effect on the line shape at higher energies because of its location at low energy and relatively smaller width and intensity. For example, in this case the peak subtracted out occurred at 4.6 meV with a FWHM of 1.6 meV and an intensity of about 20% of the main peak.

Shown in the bottom half of Fig. 5 are the calculated line shapes for the same phonon at temperatures between 10 and 75 K from GS. Comparison with our experimental line shapes immediately suggests that, both in terms of peak position (see also Fig. 1) and line shape, the calculation which utilizes Γ(SCH) is in better agreement with the data than that using SCH + C frequencies. In the former case cubic anharmonicity is treated as a perturbation on SCH frequencies when computing $S(\mathbf{Q},\omega)$. The SCH + C approximation goes one step further by using the frequencies obtained in this process to calculate the anharmonic terms $(S_{12}(\mathbf{Q},\omega),S_2(\mathbf{Q},\omega))$ and phonon damping. As was pointed out by GS, the effect of cubic anharmonicity is to lower the one-phonon frequencies relative to the SCH values. This has the effect that multiphonon terms in the SCH + C approximation also become important at lower frequencies, and in a case such as the longitudinal phonon in Fig. 5, the one-phonon peak becomes more obscured than when using the higher SCH

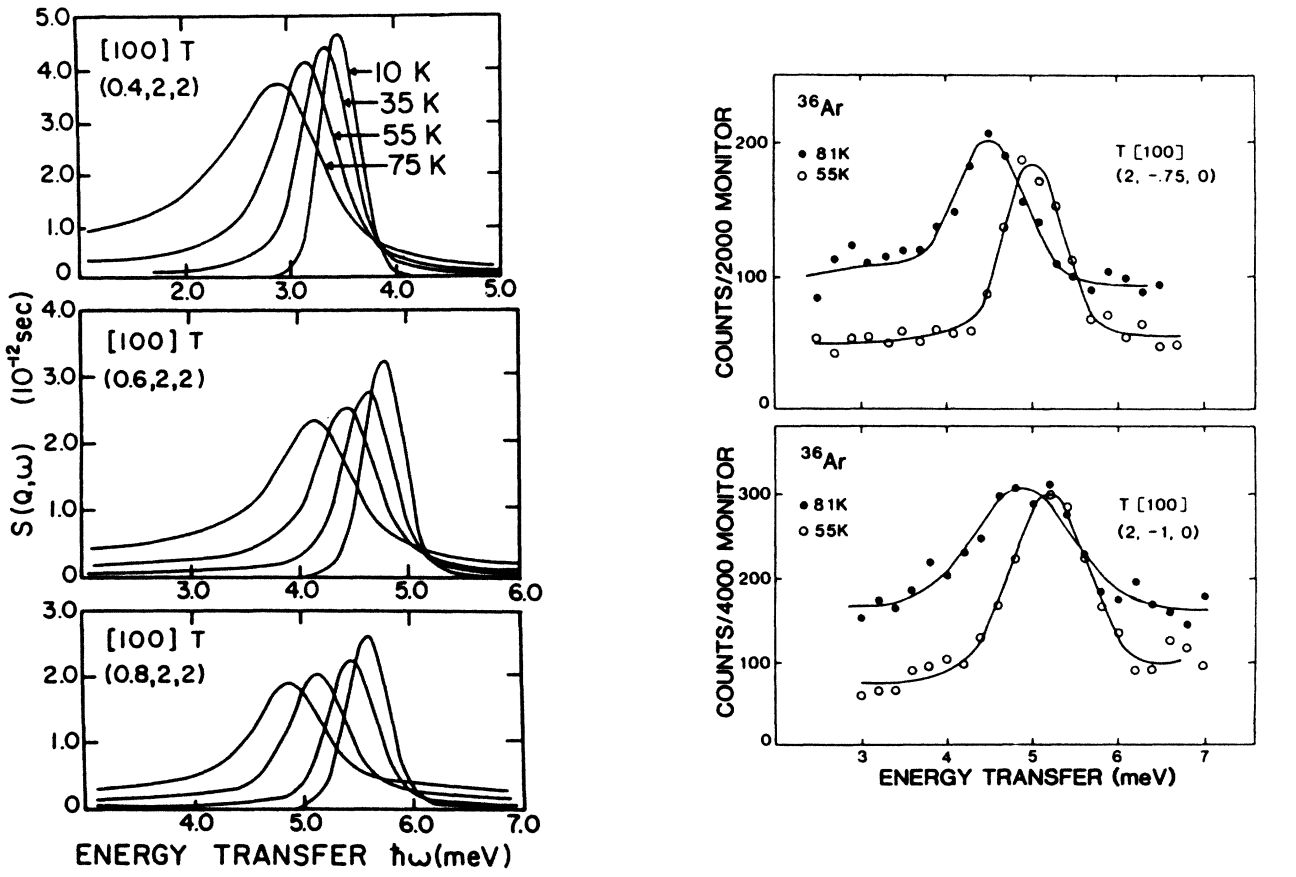

FIG. 3. Line shapes for T[100] phonons at different temperatures and wave vectors. The results of the SCH + C calculation (Fig. 14 of Ref. 10) are shown on the left and present experimental results at 55 and 81 K on the right. Solid lines in the experimental data represent fits as discussed in the text.

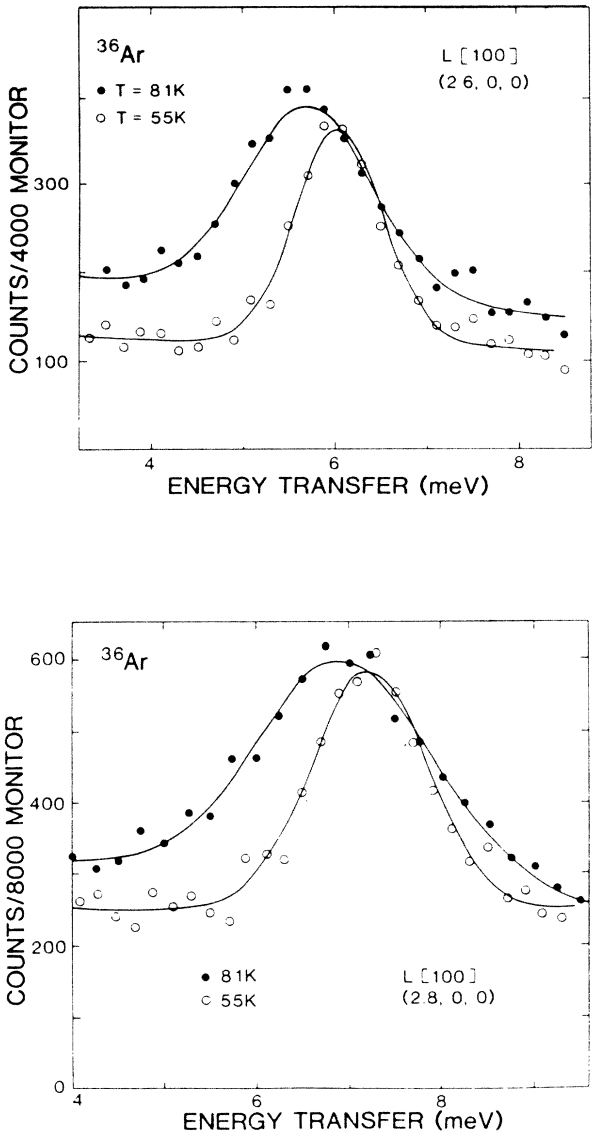

FIG. 4. Experimental line shapes for L[100] phonons at 55 and 81 K. Solid lines represent fits to the data.

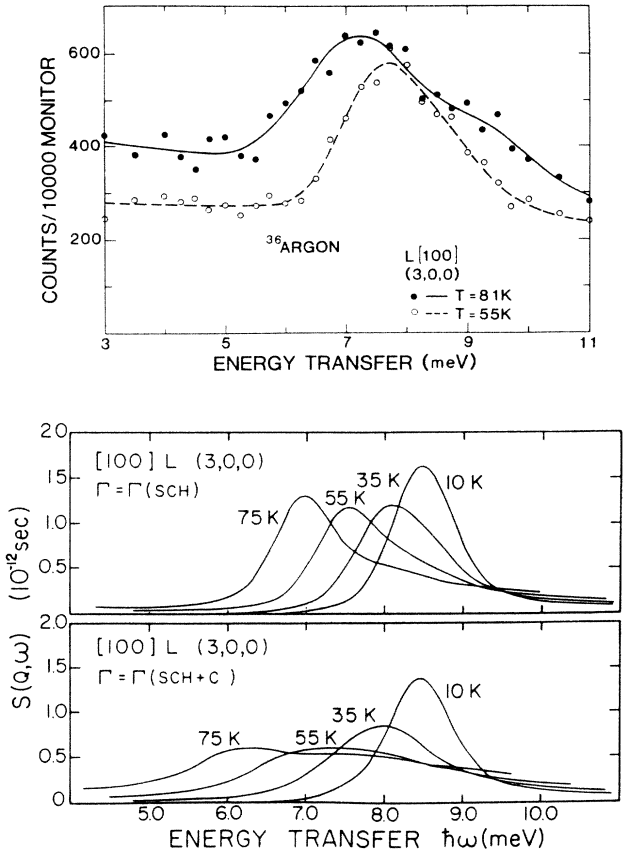

FIG. 5. Observed and calculated (Fig. 7 in Ref. 10) line shapes for the L[100] mode at the zone boundary (3,0,0) as a function of temperature. Theoretical results shown use either SCH (upper part) of SCH + C frequencies in the computation of the one-phonon width Γ and the two-phonon scattering, S_2.

frequencies. Finally, it would appear that the multiphonon terms that give rise to the shoulder at high energy in the phonon group in Fig. 5 are more strongly temperature dependent than either approximation shown in the lower half of this figure.

IV. CONCLUSIONS

The foregoing discussion has shown, in our opinion, how strictly current computational approaches to the lattice dynamics of simple anharmonic solids can be evaluated provided appropriate experimental data is available. We will not repeat in this section individual conclusions on these comparisons made above, but would simply like to point out that both the self-consistent phonon calculations and MD simulations referred to by us may well be improved in different ways. In the case of the MD work, the use of a more realistic potential than the Mie-Lennard-Jones (12-6) potential may result in better agreement with the experimental frequencies. The SCH and SCH + C calculations, on the other hand, not only need to be made fully self-consistent (as pointed out by the authors[10]) but may, at high temperatures, also profit from taking hard-core effects into account explicitly. However, we should add, that in any case we consider the general agreement of either computation with our results both on line shapes and frequencies of such an anharmonic system quite remarkable.

ACKNOWLEDGMENTS

The authors would like to thank Dr. H. R. Glyde and Dr. M. L. Klein for valuable discussions. The work at Brookhaven National Laboratory was supported by the Office of Basic Energy Sciences, U. S. Department of Energy under Contract DE-AC02-76CH00016.

[1]B. M. Powell and G. Dolling, in *Rare Gas Solids,* edited by M. L. Klein and J. A. Venables (Academic, New York, 1976), Vol. II and references contained therein.

[2]M. L. Klein and T. R. Koehler, in *Rare Gas Solids,* edited by M. L. Klein and J. A. Venables (Academic, New York, 1976), Vol. I, pp. 301—381, and references contained therein.

[3]H. R. Glyde, see Ref. 2, pp. 382—504, and references therein; W. Koehler in *Dynamic Properties of Solids,* edited by G. K. Horton and A. A. Maradudin (North-Holland, Amsterdam, 1975).

[4]J. Skalyo, Jr. and Y. Endoh, Phys. Rev. B **7**, 4670 (1973).

[5]N. A. Lurie, G. Shirane, and J. Skalyo, Jr., Phys. Rev. B **9**, 2661 (1974).

[6]L. Bohlin and T. Hogberg, J. Phys. Chem. Solids **29**, 1805 (1968).

[7]H. R. Glyde and V. V. Goldman, J. Low Temp. Phys. **25**, 601 (1976).

[8]W. M. Collins and H. R. Glyde, Phys. Rev. B **17**, 2766 (1978).

[9]W. M. Collins and H. R. Glyde, Phys. Rev. B **18**, 1132 (1978).

[10]H. R. Glyde and M. G. Smoes, Phys. Rev. B **22**, 6391 (1980).

[11]J. P. Hansen and M. L. Klein, Phys. Rev. B **13**, 878 (1976).

[12]J. Eckert, W. Thomlinson, and G. Shirane, Phys. Rev. B **16**, 1057 (1977); W. Thomlinson, J. Eckert, and G. Shirane, *ibid.* **18**, 1120 (1978).

[13]H. R. Glyde, Can. J. Phys. **52**, 2281 (1974).

[14]Y. Fujii, N. A. Lurie, R. Pynn, and G. Shirane, Phys. Rev. B **10**, 3647 (1974).

[15]See, for example, J. Skalyo, Jr., Y. Endoh, and G. Shirane, Phys. Rev. B **9**, 1797 (1974).

[16]R. Pynn and S. A. Werner, The Studsvik Science Research Laboratory, Nykoping, Sweden, Report No. AE-FF-112, 1970 (unpublished); S. A. Werner and R. Pynn, J. Appl. Phys. **42**, 4736 (1971).

[17]G. Gilat and R. J. Raubenheimer, Phys. Rev. **144**, 390 (1966).